

AD 609794
BRL R 1259

BRL

AD

BRL R 1259

REPORT
NO. 1259

SHOCK COMPRESSION OF PLEXIGLAS AND POLYSTYRENE

By G. E. Hauver
A. Melani

COPY	2	OF	3	<i>34 P</i>
HARD COPY				\$. 2.00
MICROFICHE				\$. 0.50

AUGUST 1964

U. S. ARMY MATERIEL COMMAND
BALLISTIC RESEARCH LABORATORIES
ABERDEEN PROVING GROUND, MARYLAND

DDC
RECEIVED
DEC 24 1964
DDC-IRA C

ARCADE COPY

Destroy this report when it is no longer needed.
Do not return it to the originator.

DDC AVAILABILITY NOTICE

Qualified requesters may obtain copies of this report from DDC.

The findings in this report are not to be construed as
an official Department of the Army position, unless
so designated by other authorized documents.

BALLISTIC RESEARCH LABORATORIES

REPORT NO. 1259

AUGUST 1964

SHOCK COMPRESSION OF PLEXIGLAS AND POLYSTYRENE

G. E. Hauver
A. Melani

Terminal Ballistics Laboratory

RDT & E Project No. 1M014501A33E

ABERDEEN PROVING GROUND, MARYLAND

BALLISTIC RESEARCH LABORATORIES

REPORT NO. 1259

GEHauver/AMelani/film
Aberdeen Proving Ground, Md.
August 1964

SHOCK COMPRESSION OF PLEXIGLAS AND POLYSTYRENE

ABSTRACT

Hugoniot curves for Plexiglas and polystyrene have been established experimentally using optical and polarization techniques. Both Hugoniots show evidence of a phase transition, although the polystyrene transition is more clearly defined than that of Plexiglas. Sep. polarization studies support the existence of both transitions. In the transitions, it is noted that the rarefaction velocity becomes equal to the shock velocity. The nature of the transitions is presently unknown.

TABLE OF CONTENTS

	Page
ABSTRACT.	3
TABLE OF SYMBOLS.	7
I. INTRODUCTION.	9
II. DETERMINATION OF HUGONIOT CURVES.	9
III. EXPERIMENTAL METHODS.	12
Explosive-Buffer Systems.	12
Streak-Camera Techniques.	14
Shock-Polarization Technique.	16
IV. RESULTS AND DISCUSSION.	21
V. SUMMARY	30
ACKNOWLEDGMENT.	30
REFERENCES.	33
DISTRIBUTION LIST	35

TABLE OF SYMBOLS

r	Shock curvature near a lateral boundary - millimeter (mm)
t	Time interval - microsecond (μsec)
$(t_2 - t_0)$	Time duration of a polarization signal - μsec
Δt	Risetime - μsec
u	Particle velocity in a shock wave - millimeter per microsecond (mm/ μsec)
u_f	Free-surface velocity - mm/ μsec
u_r	Particle velocity due to a rarefaction - mm/ μsec
w	Specimen diameter - mm
x	Specimen thickness - mm
x_1	Standoff distance - mm
x_2	Thin-plate thickness - mm
c	Rarefaction velocity - mm/ μsec
P	Pressure - kilobar (kbar)
T	Transit time through a specimen - μsec
U	Shock velocity - mm/ μs
U_s	Shock velocity in a buffer plate - mm/ μsec
V	Specific volume - cubic centimeter per gram (cc/g)
V_0	Specific volume at zero pressure - cc/g
α	Angle between the transmitted shock and the interface - degree
α_B	Angle between the incident shock and the interface - degree

I. INTRODUCTION

Although plastics are widely used in shock-wave investigations, a recent survey^{1*} shows a lack of extensive Hugoniot data. Two Hugoniot curves for Plexiglas have been reported^{2,3}, but they are not in complete agreement; a Hugoniot curve for polystyrene has also been reported⁴, but it does not extend to pressures above 60 kilobars. The Ballistic Research Laboratories conducted two series of tests to establish the Hugoniot curves for Plexiglas and polystyrene over the pressure range from approximately 20 to 300 kilobars. The first series of tests, conducted with optical techniques, established Hugoniot curves for both plastics, although it provided more data for Plexiglas. The second series of tests, conducted with a shock-induced polarization technique, used the established Plexiglas Hugoniot as a standard and obtained additional Hugoniot data for polystyrene.

Section II of this report discusses the methods used to determine Hugoniot curves, and Section III describes the experimental procedures used for the measurements. The results of the measurements are presented and discussed in Section IV, and summarized in Section V.

II. DETERMINATION OF HUGONIOT CURVES

The thermodynamic states that can be reached by shock-wave compression of a material define a curve in the pressure-volume plane called the Hugoniot. The experimental determination of the Hugoniot curve usually involves measuring the shock velocity, U , and the free-surface velocity, u_f , that result from the application of a constant pressure to one surface of a suitable test specimen. The free-surface velocity is the sum of u , the particle velocity of the shock wave, and u_r , the particle velocity due to the rarefaction wave that releases the pressure, i.e., $u_f = u + u_r$. If the material returns to its original density when the pressure returns to zero, $u = u_r$, the well-known approximation, $u = u_f/2$, applies. The pressure, P , and the specific volume, V , can then be calculated from the

* Superscript numbers denote references found on page 33.

Rankine-Hugoniot equations,

$$\left[P = Uu/V_0 \right]$$

and

$$\left[V = V_0(U - u)/U \right],$$

where V_0 is the specific volume of the unshocked material.

If the material does not return to its original density (because of the residual temperature) when the pressure returns to zero, $u \neq u_f/2$. In this case, u_r must be evaluated in order to obtain u from the measured free-surface velocity. For plastics, it was anticipated that u_r might be significantly different from u at high pressures; it is not certain that the assumptions usually used to calculate u_r are applicable. Therefore, in the Ballistic Research Laboratories' tests with Plexiglas and polystyrene, graphical solutions⁵ were used in order to avoid measuring u_f for either plastic.

In the first series of the Ballistic Research Laboratories' tests, Plexiglas and polystyrene specimens were mounted on metal buffer plates through which plane shock waves were propagated. The free-surface velocity of the buffer and the average shock velocity through the plastic specimens were measured. The instantaneous shock velocity at the buffer-plastic interface was obtained from the average shock velocity by an attenuation correction, except for certain experiments in which the shock velocity was constant. The particle velocity of the buffer was determined from the measured free-surface velocity by calculated u_r/u ratios reported in Reference (5). In a graphical solution, illustrated in Figure 1, the buffer Hugoniot was reflected through the points (P,u) and $(u_f + 2u)/2$ at zero pressure in an effort to bring the reflected curve into close agreement with the adiabat in the region where Hugoniot points were obtained for the plastics. The intersection of the reflected curve with the U/V_0 line for each plastic provided Hugoniot points. In the first series of tests, more points were obtained for Plexiglas than for polystyrene, establishing the Plexiglas Hugoniot with greater reliability.

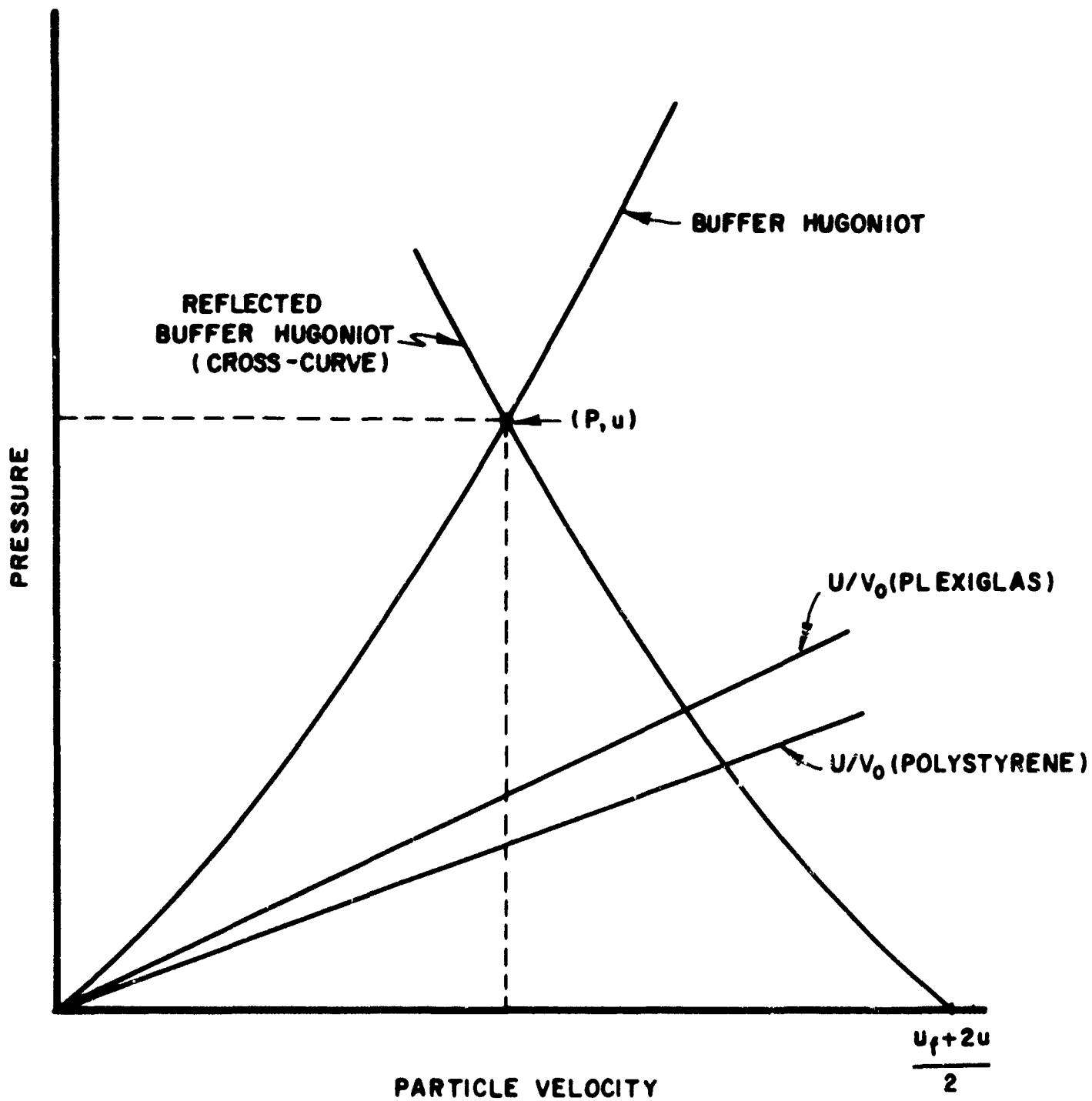


FIGURE 1. Graphical solution. Buffer Hugoniot is known, and measured quantities are: buffer free-surface velocity; Plexiglas shock velocity; and polystyrene shock velocity. Hugoniot points are at intersections of U/V_0 lines with the cross curve.

In the second series of tests, additional Hugoniot points were obtained for polystyrene. Average shock velocities through Plexiglas and polystyrene specimens were calculated from shock-transit times obtained by simultaneous polarization measurements. The Plexiglas Hugoniot curve, established in the first series of tests, was used to determine the pressure-particle velocity state of the Plexiglas from the shock velocity. As shown in Figure 2, the buffer Hugoniot was reflected through the (P,u) point on the Plexiglas Hugoniot. The Hugoniots of the two plastics are together in the pressure-particle velocity plane, so the reflected curve should closely approximate the adiabat in the vicinity of the intersection with the U/V_0 line for polystyrene.

III. EXPERIMENTAL METHODS

Plexiglas II UVA specimens with a density of 1.18 grams per cubic centimeter and ordinary amorphous polystyrene with a density of 1.05 grams per cubic centimeter were used for all measurements. Explosive-buffer systems provided the shock pressures. In the first series of tests, shock and free-surface velocities were measured by streak-camera techniques. In the second series, shock velocities were measured by a polarization technique.

Explosive-Buffer Systems

Shock pressures were produced by detonating an explosive charge consisting of a plane-wave lens followed by a base charge of TNT, Composition B, 9404 or 75/25 Octol. Plane-wave lenses were the two-explosive type⁶, and 102 mm diameter and 152 mm diameter sizes were used. Base charges for the small lenses were 25 mm thick and 102 mm in diameter, and base charges for the larger lenses were 51 or 102 mm thick and 190 mm in diameter.

Highest pressures were achieved with a 1.57 mm thick aluminum or titanium buffer impacted by a 3.18 mm thick aluminum plate that was accelerated through approximately 25 mm. Lower pressures were produced by detonating the explosive in direct contact with a buffer, and pressure

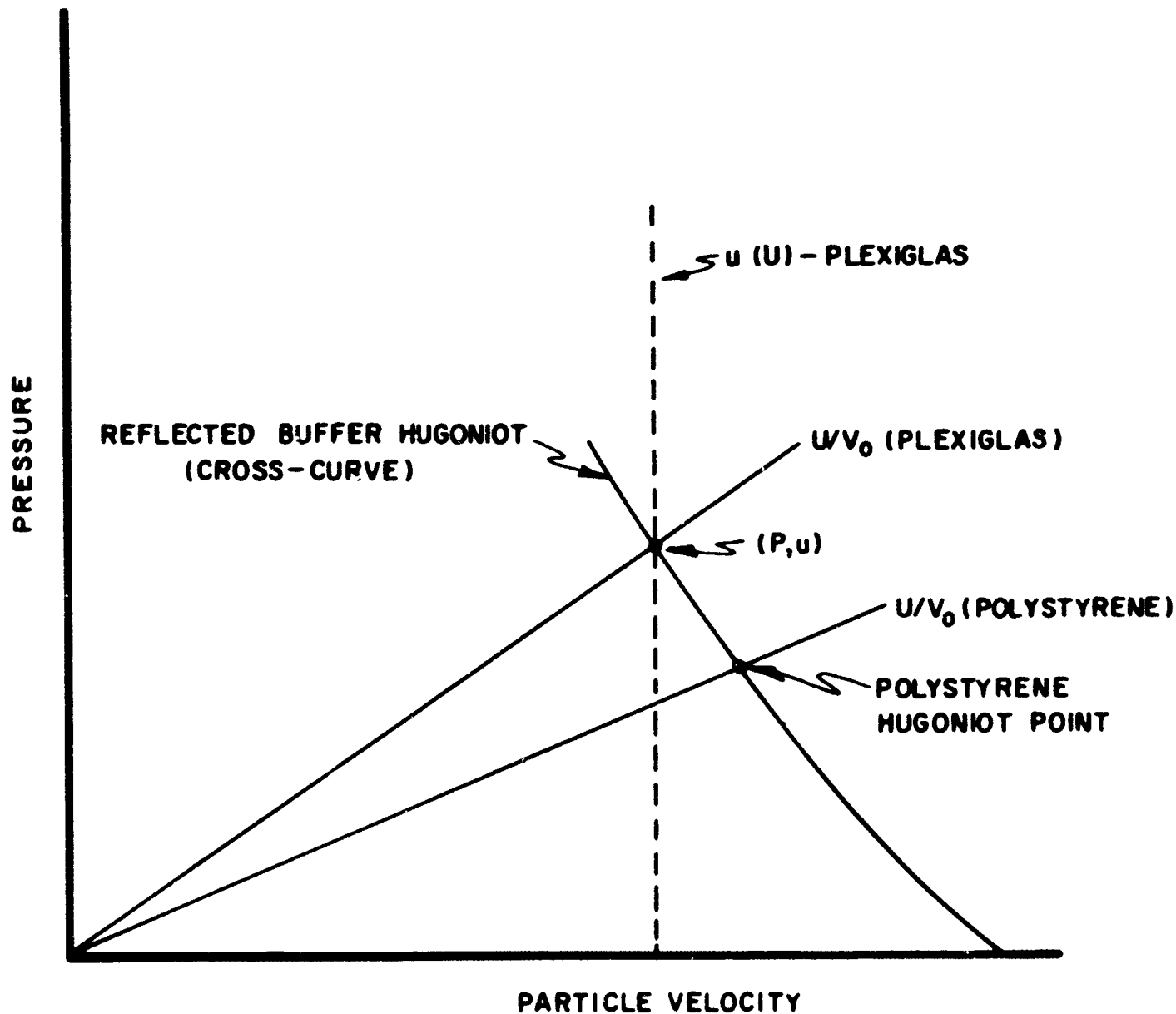


FIGURE 2. Graphical solution. Plexiglas and buffer Hugoniots are known. Measured quantities are Plexiglas and polystyrene shock velocities.

was varied by the choice of base-charge explosive, buffer metal and buffer thickness. Lowest pressures were achieved with laminated buffers which reduced the pressure by impedance mismatch between laminations.

Streak-Camera Techniques

Argon-flash gaps and changes in reflectivity caused by a shock were used to detect surface displacement for streak-camera measurements of free-surface velocity. For the argon-gap technique, three gaps were used for each velocity measurement. Two gaps detected shock arrival at the free surface, and a centrally located gap detected the free surface after a maximum displacement of 3.18 mm. Gaps were spaced to prevent interaction, but the spacing could introduce timing error if the shock front was curved in the area of the measurement. Consequently, a reflectivity technique was introduced to reduce timing error due to curvature. Figure 3 shows the basic reflectivity technique. A 0.51 mm thick plate of the buffer material was accurately positioned above the free surface of the buffer. The buffer surface and the upper surface of the thin plate were lightly abraded with 27 μ aluminum oxide by an airbrasive unit to diffuse reflected light. The surfaces were illuminated by an explosive-argon source, and shock arrival at the free surface produced a well-defined decrease in reflectivity, except at low pressures. (The lower limit of usefulness depends upon the material. For 2024 aluminum, the lower limit is approximately 125 kilobars.) Free-surface impact on the thin plate produced a shock which decreased the reflectivity when it interacted with the abraded surface. The free-surface velocity of the buffer is given by $u_f = x_1 / (t - x_2/U)$, where t is the measured time interval, U is the shock velocity in the thin plate, and x_1 and x_2 are the standoff and thin-plate thickness, respectively. The term x_2/U is small compared to t , and u_f is relatively insensitive to the initial estimate for U . The value for U can usually be estimated with a reasonable accuracy, and both U and u_f are improved by iteration.

This reflectivity technique was modified to measure the shock velocity through Plexiglas and polystyrene specimens mounted on a buffer surface. The free surfaces of the buffer and plastics were lightly abraded with

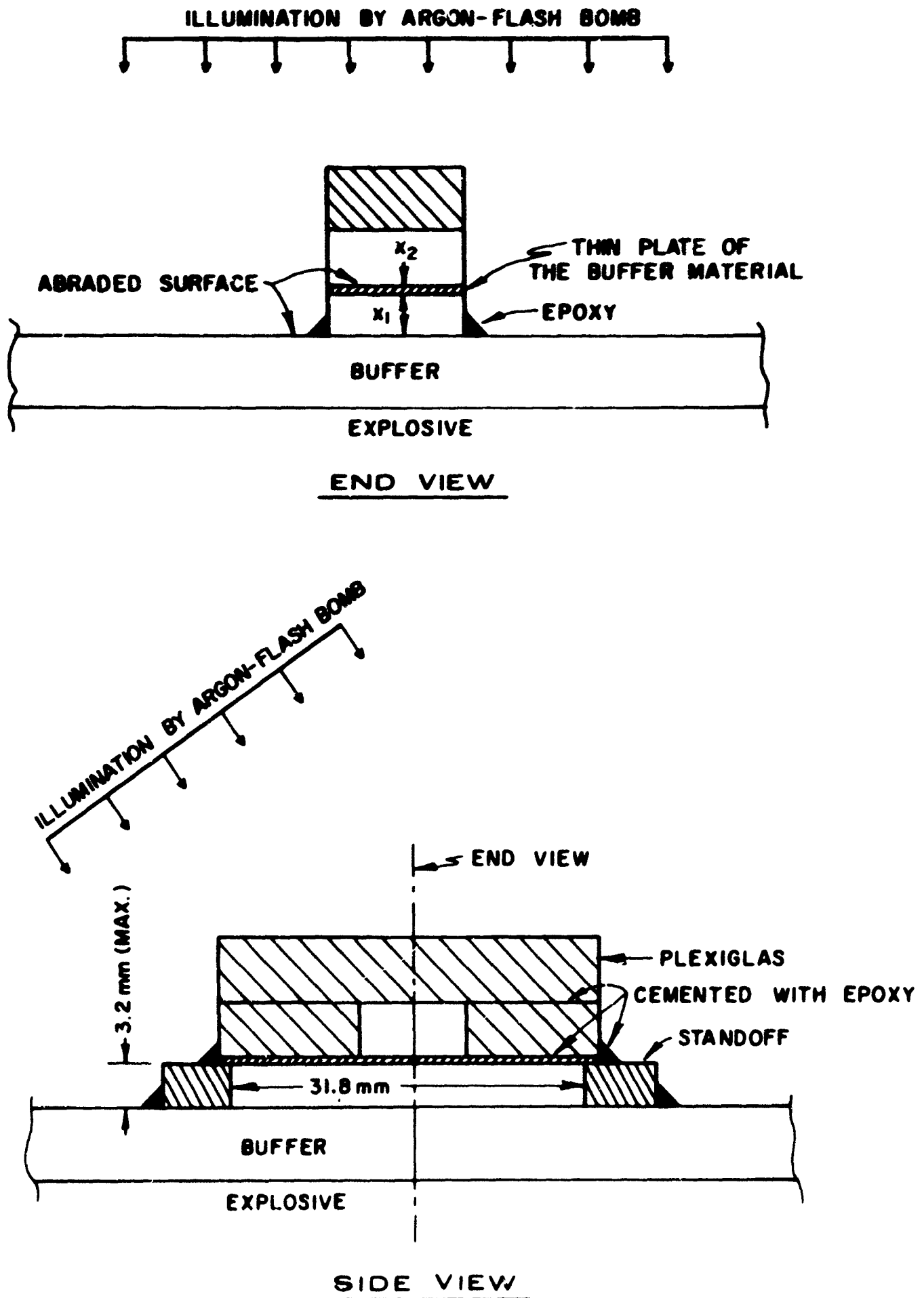


FIGURE 3. Experimental arrangement for measuring free-surface velocity by reflectivity changes caused by shock.

27 μ aluminum oxide, and the abraded surface of the plastics was coated with aluminum by vacuum evaporation. The time interval between changes in reflectivity caused by the shock at the free surfaces of the buffer and plastics was measured and used to calculate the average shock velocity. Specimens with thicknesses of 3.18, 6.35, and 9.52 mm were included on many tests, and diameter-to-thickness ratios were selected to provide a central area, at least 6 mm in diameter, that was undisturbed by the rarefaction from the lateral boundary. The average shock velocities through the different thicknesses were extrapolated to the interface for the instantaneous velocity needed to establish the U/V_0 line in a graphical solution. The measurements showed that shock-velocity attenuation was approximately 1 percent per 1.57 millimeters with the large charges and 1.5 percent per 1.57 millimeters with the small charges, and it did not appear to be significantly dependent upon the initial interface pressure. For tests in which attenuations were not measured, these attenuation corrections were applied to the average shock velocities. No corrections were applied in plate-impact tests because plate dimensions should have prevented the rarefaction from overtaking the shock in the plastic specimens.

Shock-Polarization Technique

Average shock velocities through specimens of Plexiglas and polystyrene were also obtained by shock-polarization measurements. Figure 4 shows the experimental arrangement. Plastic specimens, 3.18 mm thick and 12.70 mm in diameter, were placed between parallel electrodes. The metal buffer served as one electrode, and a vacuum-evaporated copper coating served as the electrode on the opposite surface of each specimen. The electrodes were connected through a 93-ohm resistor, and the displacement current generated by the shocked specimen was detected by the voltage drop across the resistor.

Figure 5 shows an idealized current-time polarization signal. The shock front arrives at the buffer-specimen interface at time t_0 . If the shock front is plane and normally incident to the interface, experience has shown that the risetime of the signal is the risetime of the recording

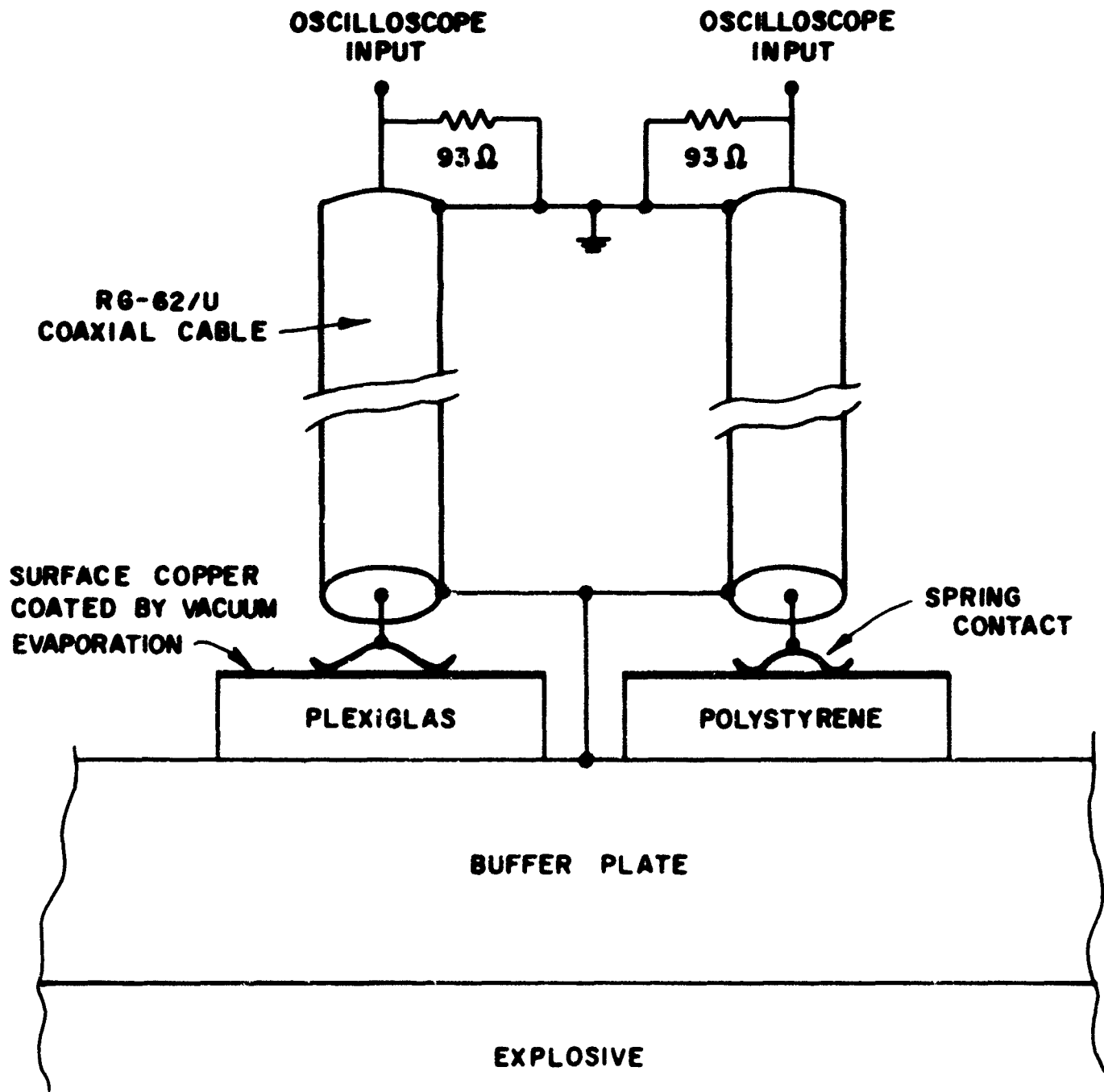
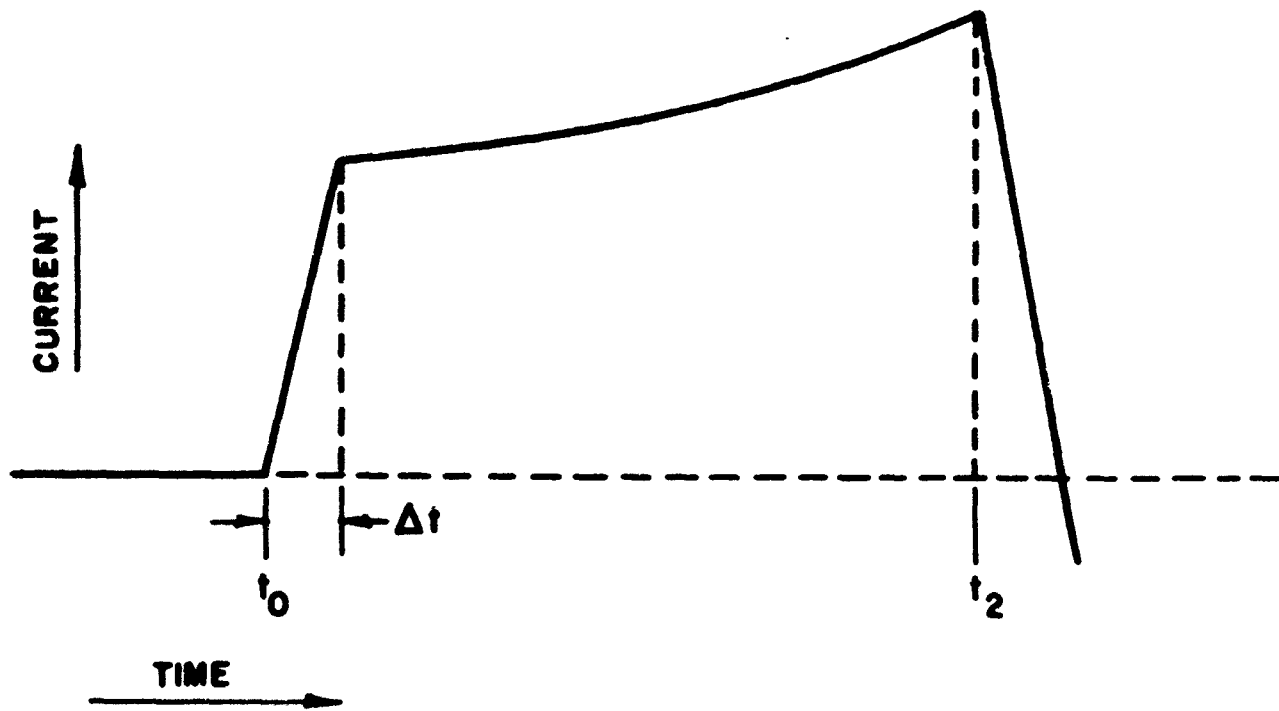


FIGURE 4. Experimental arrangement for measuring shock velocity by shock polarization.



t_0 : SHOCK ARRIVES AT FIRST BUFFER-SPECIMEN INTERFACE
 t_2 : SHOCK ARRIVES AT SECOND SPECIMEN-BUFFER INTERFACE
 Δt : SIGNAL RISE TIME

FIGURE 5. Idealized polarization signal.

instrument. At time t_2 , the shock front arrives at the second specimen-electrode interface. The time interval $(t_2 - t_0)$ is the transit time of the shock wave.

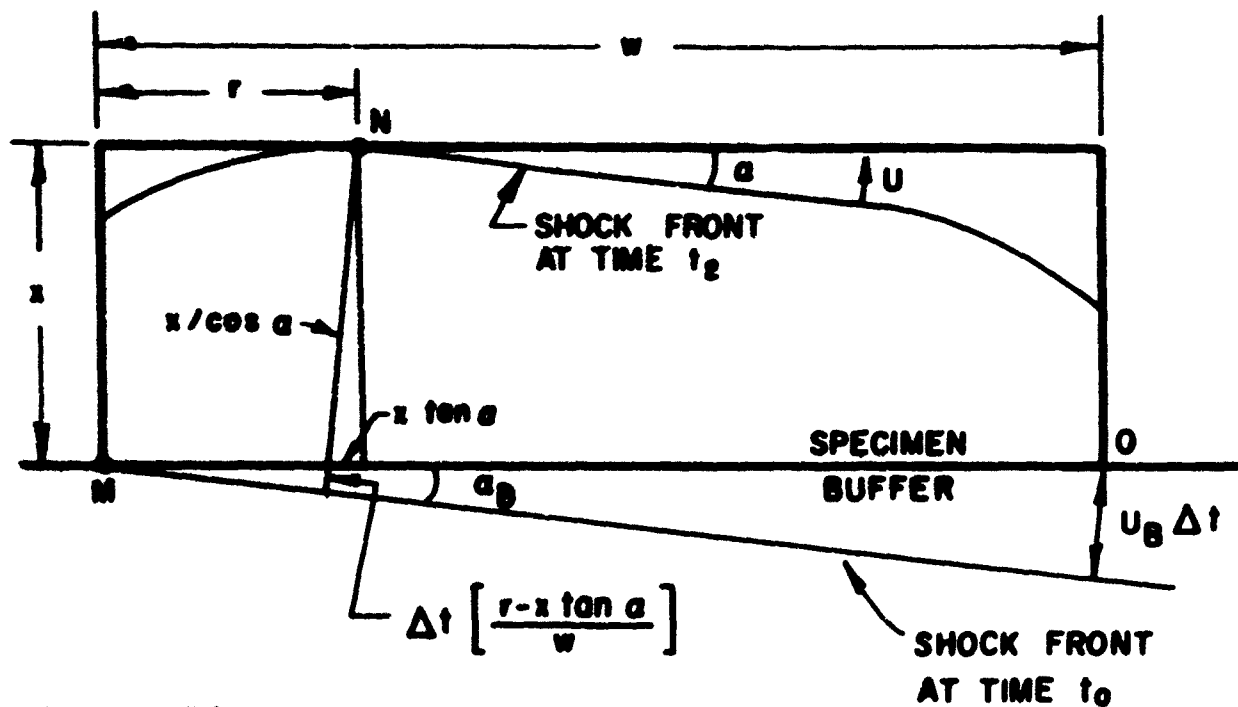
The assumption of a plane, normally incident shock front, is usually not valid. Explosively generated "plane" shock waves usually have measurable curvature and obliquity. In these tests, the small specimen diameter reduced the influence of curvature and obliquity. To further reduce the influence of curvature, the specimen was placed on the buffer in a location where wave-shape measurements indicated minimum curvature. Figure 6 illustrates the situation in which an unconfined cylindrical specimen, in direct contact with a buffer, is impacted from the buffer by a plane, oblique shock front. The shock approaches the interface at an angle α_B . At time t_0 , the shock arrives at M. The shock travels an additional distance, $U_B \Delta t$, arriving at O. In the specimen, the shock front is at an angle α . The rarefaction, which originates at the lateral boundary, relieves the compression and causes the shock front to curve back in the region near the boundary. Because of curvature, the shock front arrives at the free surface first at N, a radial distance r from the lateral boundary. The time of arrival at N is t_2 . From the geometry of the situation, it is evident that the transit time, T , is

$$T = (t_2 - t_0) - \Delta t(r - x \tan \alpha)/w . \quad (1)$$

The distance traveled through the specimen is $x/\cos \alpha$, so the shock velocity is $x/T \cos \alpha$. The angle α is usually less than one degree. Therefore, $x \tan \alpha \ll r$ since $x \approx r$; $x/\cos \alpha \approx x$, and the shock velocity is closely approximated by the equation,

$$U = x / \left[(t_2 - t_0) - \Delta t(r/w) \right] . \quad (2)$$

The time interval $(t_2 - t_0)$ and the risetime Δt were measured from the polarization signal; x and w were measured specimen dimensions. The reflectivity technique, used to measure shock velocity in the first series of



- r : CURVATURE
 w : SPECIMEN DIAMETER
 M : POINT WHERE SHOCK FRONT FIRST ENTERS SPECIMEN
 N : POINT WHERE SHOCK FRONT FIRST ARRIVES AT SPECIMEN FREE SURFACE
 O : POINT DIAMETRICALLY OPPOSITE POINT M
 U : SHOCK VELOCITY IN SPECIMEN
 U_B : SHOCK VELOCITY IN BUFFER
 x : SPECIMEN THICKNESS
 α : ANGLE BETWEEN THE TRANSMITTED SHOCK AND THE INTERFACE
 α_B : ANGLE BETWEEN THE INCIDENT SHOCK AND THE INTERFACE
 TIMES t_0 AND t_2 , AND TIME INTERVAL Δt , ARE INDICATED IN FIG. 5

FIGURE 6. Geometry of the situation in which an unconfined cylindrical specimen is impacted at the buffer-specimen interface by a plane, oblique shock front.

tests, also provided curvature as a function of shock velocity. By the initial estimate, $U = x/(t_2 - t_0)$, a value of r was selected for use in Equation (2); the values of r and U were improved by iteration.

IV. RESULTS AND DISCUSSION

Hugoniot points for polystyrene are listed in Table I and plotted in Figure 7. The data indicate a phase transition in the vicinity of 180 kilobars. Curve I is a linear least-squares fit to the data below the transition and is represented by the equation,

$$U = 2.48 + 1.63u . \quad (3)$$

The data from streak-camera measurements is displaced slightly below the data from polarization measurements. However, all data points were assigned equal weight to obtain Curve I because the methods of measurement are believed to be equally reliable. Curve II is a linear least-squares fit to the data above the transition and is represented by the equation,

$$U = 3.96 + 0.96u . \quad (4)$$

(Although in the data above the transition is presented as linear, the range of values is too short to confirm linearity.) Shock wave compression data for polystyrene, based on the linear least-squares fits, is listed in Table II.

The existence of a polystyrene transition was initially doubted because it occurred between the highest pressure usually achieved with direct contact systems and the lowest pressure usually achieved with plate impact. Tests were conducted in an effort to reveal an experimental flaw that might introduce a discontinuity. Plate-impact tests were conducted at pressures below the transition and substantiated the data obtained with buffer systems. Optical and polarization measurements gave no indication of either spalling or breakup which might have influenced the plate-impact tests at high pressures. Tests conducted in vacuum indicated that the air shock driven ahead of the flying-plate did not significantly

TABLE I
EXPERIMENTAL VALUES OF
SHOCK AND PARTICLE VELOCITY FOR POLYSTYRENE

<u>Streak-Camera Measurements</u>		<u>Polarization Measurements</u>	
<u>U</u>	<u>u</u>	<u>U</u>	<u>u</u>
3.91	0.92	3.38	0.57
5.26	1.73	3.59	0.70
5.35	1.81	3.87	0.87
5.85	2.15	3.93	0.88
6.12	2.29	3.95	0.88
6.37	2.38	3.96	0.90
6.46	2.48	3.97	0.88
6.75	2.75	4.34	1.11
6.87	3.00	4.42	1.31
7.15	3.32	4.47	1.22
7.17	3.39	4.80	1.43
7.26	3.49	5.09	1.46
7.28	3.40	5.16	1.62
7.31	3.45	5.69	2.01
7.31	3.52	5.72	1.98
7.34	3.46	5.80	2.05
		5.82	2.05
		6.03	2.13
		6.16	2.23
		6.24	2.28
		6.36	2.40
		6.58	2.48
		6.73	2.92
		6.87	3.01

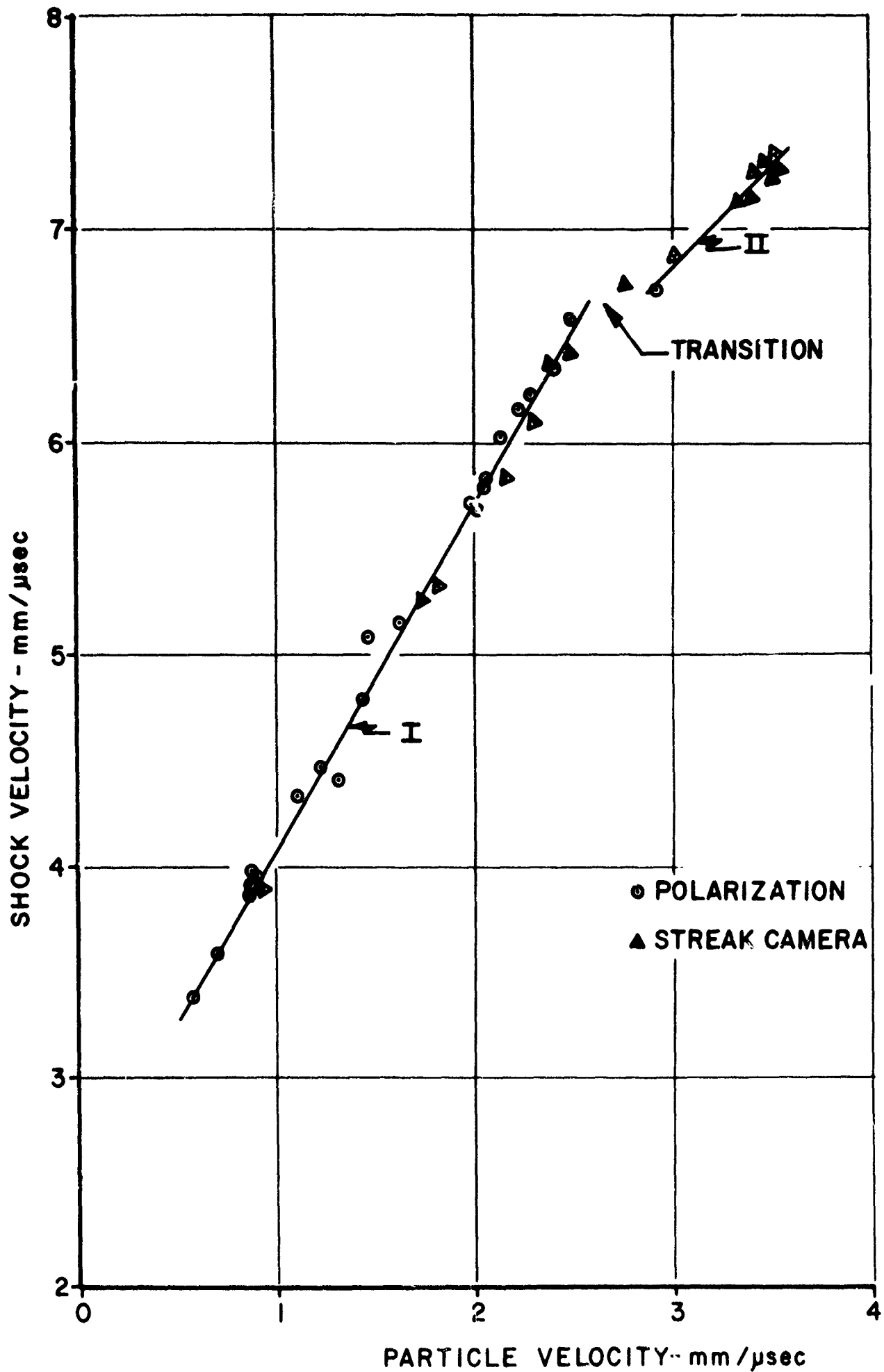


FIGURE 7. Shock velocity - particle velocity relationship for polystyrene.

TABLE II
SHOCK-WAVE COMPRESSION DATA FOR POLYSTYRENE

<u>u</u>	<u>U</u>	<u>P</u>	<u>v/v₀</u>
0.80	3.78	31.8	0.788
0.90	3.95	37.3	0.772
1.00	4.11	43.2	0.757
1.10	4.27	49.3	0.742
1.20	4.44	55.9	0.730
1.30	4.60	62.8	0.717
1.40	4.76	70.0	0.706
1.50	4.92	77.5	0.695
1.60	5.09	85.5	0.686
1.70	5.25	93.7	0.676
1.80	5.41	102	0.667
1.90	5.58	112	0.659
2.00	5.74	121	0.652
2.10	5.90	130	0.644
2.20	6.07	140	0.638
2.30	6.23	150	0.631
2.40	6.39	161	0.624
2.50	6.56	172	0.619
2.60	6.73	184	0.614
<u>TRANSITION</u>			
2.90	6.74	205	0.570
3.00	6.84	215	0.561
3.10	6.94	226	0.553
3.20	7.03	236	0.545
3.30	7.13	247	0.537
3.40	7.22	258	0.529
3.50	7.32	269	0.522

influence either shock or free-surface velocity measurements. Melting of the 2024 aluminum buffer was considered as a remote possibility, although it was not expected to occur upon release from pressures as low as 450 kilobars. One test conducted with a titanium buffer confirmed the data obtained with 2024 aluminum. Buffers of 2024 aluminum were used at pressures as high as 590 kilobars, and it was anticipated that partial melting might occur between 550 and 590 kilobars. However, the highest pressure Hugoniot points do not deviate from the trend of points obtained at lower pressure where no melting was expected. Other tests confirmed the constancy of the free-surface velocity measured in plate-impact tests, and the equivalence of reflectivity and argon-gap techniques for velocity measurements. The search for experimental flaws failed to reveal any by which the transition could be refuted.

The existence of a polystyrene transition is further supported by shock-induced polarization measurements⁷ which show a sudden change in the profile of the polarization (current-time) signal between 167 and 207 kilobars. The sudden change is the result of a rapid increase in polarization and a rapid decrease in relaxation time.

Hugoniot points for Plexiglas are listed in Table III and plotted in Figure 8. If it were not for the evidence of a polystyrene transition, the data in Table III might have been fitted with a quadratic function. However, linear fits were considered, and two straight lines were found to provide a better fit to the experimental points than a quadratic. It is noted that the linear fits indicate a transition at the particle velocity that corresponds to the polystyrene transition. Curve I is a linear least-squares fit to the data below the transition and is represented by the equation

$$U = 2.68 + 1.61u . \quad (5)$$

Curve II is a linear least-squares fit to the data above the transition and is represented by the equation,

$$U = 3.51 + 1.25u . \quad (6)$$

TABLE III
EXPERIMENTAL VALUES OF
SHOCK AND PARTICLE VELOCITY FOR PLEXIGLAS

<u>U</u>	<u>u</u>	<u>U</u>	<u>u</u>
4.07	0.89	6.78	2.46
4.58	1.17	6.88	2.72
4.60	1.15	6.93	2.65
5.45	1.75	7.13	2.88
5.47	1.80	7.32	3.08
5.52	1.71	7.50	3.19
6.05	2.08	7.54	3.24
6.07	2.11	7.57	3.33
6.08	2.03	7.58	3.28
6.08	2.16	7.62	3.28
6.09	2.20	7.62	3.32
6.15	2.10	7.62	3.35
6.16	2.12	7.64	3.28
6.46	2.34	7.66	3.25
6.48	2.38	7.77	3.36

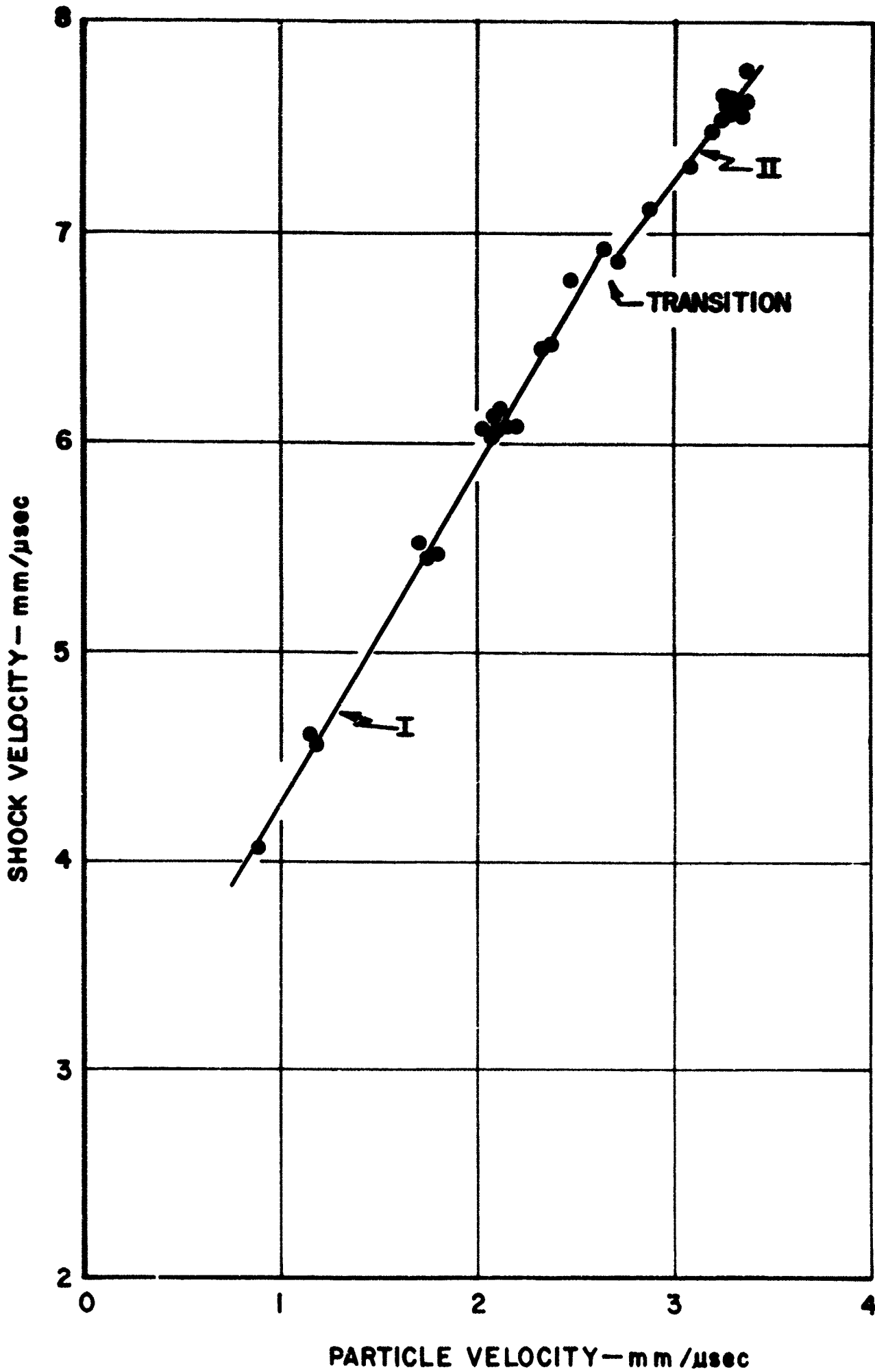


FIGURE 8. Shock velocity - particle velocity relationship for Plexiglas.

(As in the case of polystyrene, the range of values above the transition is too short to actually confirm linearity.) Shock wave compression data for Plexiglas, based on the linear least-squares fits, is listed in Table IV.

Since the shock-induced polarization signal of polystyrene suddenly changed at the transition, it was inferred that a similar change might be observed for Plexiglas. Polarization tests with Plexiglas were conducted at 267 and 295 kilobars and are reported in Reference 9. The relaxation time which had remained constant at approximately 0.70 μ second up to a pressure of 212 kilobars, had decreased to 0.25 μ second at 267 kilobars and to 0.03 μ second at 295 kilobars. The shock-induced polarization showed a corresponding increase. The polarization measurements suggested a transition beginning between 212 and 267 kilobars, which corresponded to the pressure range where Plexiglas Curves I and II indicated a transition.

For the configuration in Figure 6, it can be shown that when α is zero or negligibly small, the velocity of the rarefaction relative to the compressed material into which it propagates can be represented by the equation,

$$C = U \sqrt{\left(\frac{r}{x}\right)^2 + \left(\frac{v}{V_0}\right)^2} . \quad (7)$$

Usually, α is negligibly small and values of C can be calculated since U , V , V_0 , x , and r have been evaluated. In order to establish the significance of such calculated values of C , four control tests were performed with 2024 aluminum specimens. The values of C , calculated by Equation (7), were found to be within 4 percent of corresponding sound velocities for 2024 aluminum obtained by interpolation from Table VI of Reference 5. It was concluded that values of C , similarly calculated for Plexiglas and polystyrene, should also be close to the sound velocities.

TABLE IV
SHOCK-WAVE COMPRESSION DATA FOR PLEXIGLAS

<u>u</u>	<u>U</u>	<u>P</u>	<u>V/V₀</u>
0.90	4.13	43.9	0.782
1.00	4.29	50.6	0.767
1.10	4.45	57.8	0.753
1.20	4.61	65.3	0.740
1.30	4.77	73.2	0.727
1.40	4.93	81.4	0.716
1.50	5.10	90.3	0.706
1.60	5.26	99.3	0.696
1.70	5.42	109	0.686
1.80	5.58	119	0.677
1.90	5.74	129	0.669
2.00	5.90	139	0.661
2.10	6.06	150	0.653
2.20	6.22	161	0.646
2.30	6.38	173	0.639
2.40	6.54	185	0.633
2.50	6.70	198	0.627
2.60	6.87	211	0.622
<u>TRANSITION</u>			
2.80	7.01	232	0.601
2.90	7.13	244	0.593
3.00	7.26	257	0.587
3.10	7.39	270	0.581
3.20	7.51	284	0.574
3.30	7.63	297	0.567
3.40	7.76	311	0.562

Figures 9 and 10 show C as a function of pressure for polystyrene and Plexiglas, respectively. The values of C based on curvature measurements are indicated by circles. Figures 9 and 10 also show shock velocity as a function of pressure. For polystyrene, the experimental $C(P)$ curve goes through a maximum and intersects the $U(P)$ curve in the vicinity of the transition. In the case of Plexiglas, the experimental $C(P)$ curve intersects the $U(P)$ curve in the vicinity of the transition but does not appear to have a closely associated maximum.

The results of the rarefaction-velocity determinations suggest that $C = U$ is associated with the conditions that accompany the transitions in polystyrene and Plexiglas. The significance of this observation is not clear, and the nature of the transitions is not understood at the present time.

V. SUMMARY

Hugoniot curves for Plexiglas and polystyrene have been established experimentally, and both show evidence of phase transitions that begin at a particle velocity of approximately 2.6 millimeters per microsecond. The Plexiglas Hugoniot is represented by $U = 2.68 + 1.61u$ below the transition and by $U = 3.51 + 1.25u$ above the transition. The polystyrene Hugoniot is represented by $U = 2.48 + 1.63u$ below the transition and by $U = 3.96 + 0.96u$ above the transition. The Hugoniots define the polystyrene transition more clearly, but separate polarization studies support the existence of both transitions. It is noted that the rarefaction velocity becomes equal to the shock velocity at the transitions, but no explanation is offered. The nature of the transitions is unknown at the present time.

ACKNOWLEDGEMENT

The authors wish to thank Dr. F. E. Allison for advice and guidance during the course of the investigation.

G. E. Hauer

G. E. HAUVER

A. Melani

A. MELANI

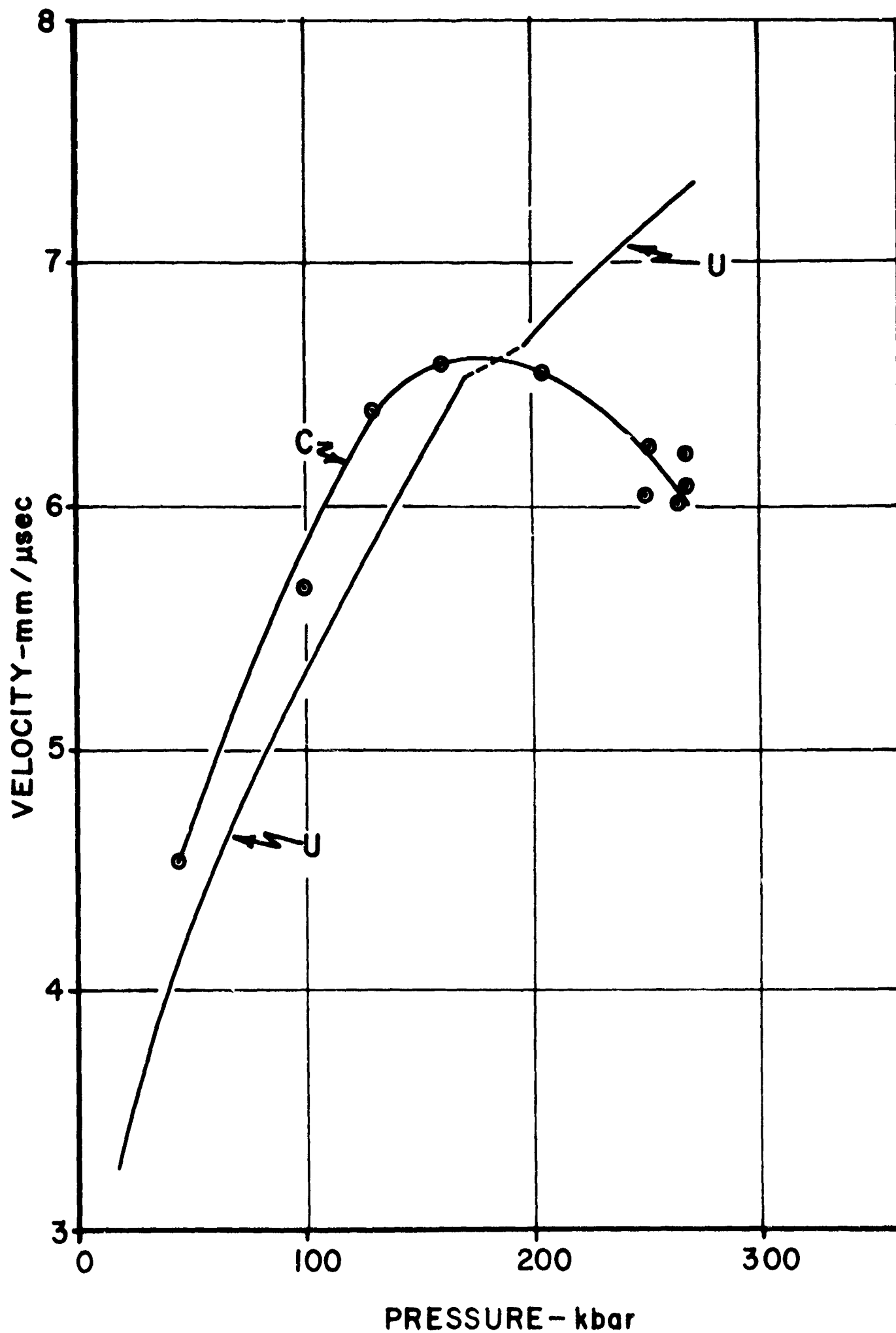


FIGURE 9. Rarefaction and shock velocity as a function of pressure for polystyrene.

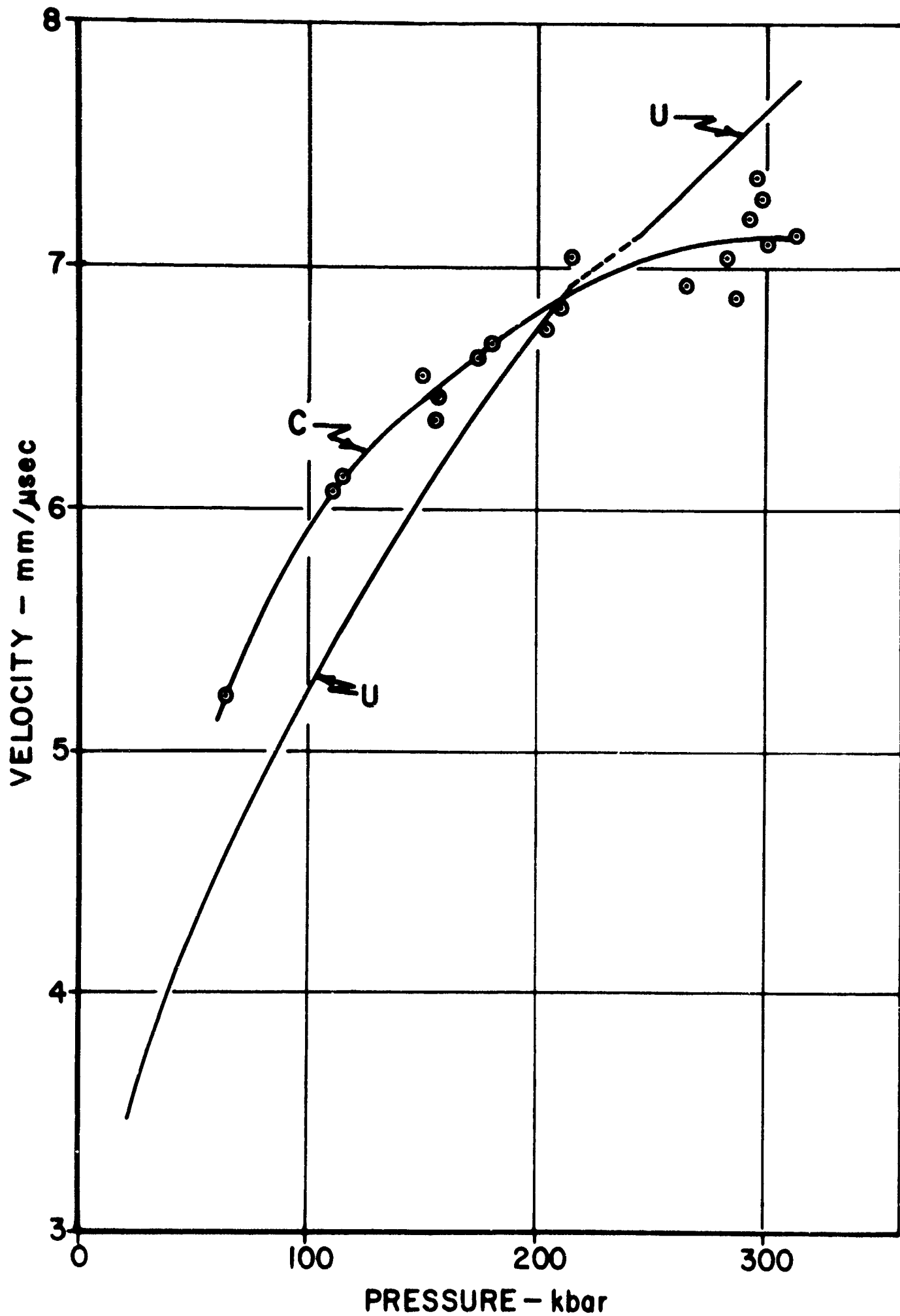


FIGURE 10. Rarefaction and shock velocity as a function of pressure for Plexiglas.

REFERENCES

1. Brush, S. G., Kraft, R., and Senkin, J. High Pressure Equation of State Bibliography and Index (1925 - 1962). University of California Radiation Laboratory, Livermore, California, UCRL-7160, January 1963.
2. Coleburn, N. L. The Dynamic Compressibility of Solids from Single Experiments Using Light Reflection Techniques. U. S. Naval Ordnance Laboratory, White Oak, Silver Spring, Maryland, NAVWEPS Report 6026, January 1961.
3. Reynolds, C. E. and Seay, G. E. Two-Wave Shock Structures in the Ferroelectric Ceramics Barium Titanate and Lead Zirconate Titanate. J. Appl. Phys., 33, 2236, July 1962.
4. Wagner, M. H., Anderson, W. H., and Kreyenhagen, K. N. Aerojet-General, Downey, California, Report AGC Plastic AR-31, March 1960. (SECRET)
5. Walsh, J. M., Rice, M. H., McQueen, R. G., and Yarger, F. L. Shock-Wave Compression of Twenty-Seven Metals. Equations of State of Metals. Phys. Rev., 108, 196-216, 15 October 1957.
6. Duvall, G. E. and Fowles, G. R. High Pressure Physics and Chemistry, Volume 2. (Edited by Bradley, R. S.), New York, Academic Press, Inc., 1963.
7. Allison, F. E. and Hauver, G. E. Shocked-Induced Polarization of Plexiglas and Polystyrene. Aberdeen Proving Ground, Maryland, BRL Report No. 1258, August 1964.

DISTRIBUTION LIST

<u>No. of Copies</u>	<u>Organization</u>	<u>No. of Copies</u>	<u>Organization</u>
20	Commander Defense Documentation Center ATTN: TIPCR Cameron Station Alexandria, Virginia 22314	1	Commanding General US Army Materials Research Agency Watertown, Massachusetts
2	Chief, Defense Atomic Support Agency ATTN: Maj. B. M. Carswell Blast and Shock Section Washington, D. C. 20301	1	Commanding Officer Army Research Office (Durham) ATTN: CRD-AA-IPL Box CM, Duke Station Durham, North Carolina 27706
1	Director of Research & Engineering (OSD) The Pentagon Washington, D. C. 20301	1	Chief of Research and Development ATTN: Army Research Office Department of the Army Washington 25, D. C.
1	Commanding General U. S. Army Materiel Command ATTN: AMCRD-RP-B Washington, D. C. 20315	1	Commander U. S. Naval Ordnance Test Station China Lake, California 93557
1	Commanding General U. S. Army Materiel Command ATTN: AMCRD-RC Washington, D. C. 20315	2	Commander U. S. Naval Ordnance Laboratory White Oak Silver Spring, Maryland 20910
1	Commanding Officer ATTN: Mr. J. Hershkowitz Picatinny Arsenal Dover, New Jersey 07801	1	Director U. S. Naval Research Laboratory Washington, D. C. 20390
1	Commanding General U. S. Army Engineering Research and Development Labs. ATTN: STINFO Branch Fort Belvoir, Virginia 22060	1	AFWL (WLL) Kirtland AFB New Mexico 87117
1	Army Research Office 3045 Columbia Pike Arlington, Virginia 22204	2	U. S. Atomic Energy Commission Los Alamos Scientific Laboratory P. O. Box 1663 Los Alamos, New Mexico
		1	U. S. Atomic Energy Commission ATTN: Technical Reports Library Washington 25, D. C.

DISTRIBUTION LIST

<u>No. of Copies</u>	<u>Organization</u>	<u>No. of Copies</u>	<u>Organization</u>
2	U. S. Atomic Energy Commission Lawrence Radiation Laboratory P. O. Box 808 Livermore, California	4	Defence Research Member Canadian Joint Staff 2450 Massachusetts Avenue, N. W. Washington, D. C. 20008
1	U. S. Department of Interior Bureau of Mines ATTN: Chief, Explosive and Physical Sciences Div. 4800 Forbes Street Pittsburgh 13, Pennsylvania		<u>Aberdeen Proving Ground</u> Chief, TIB Air Force Liaison Office Marine Corps Liaison Office Navy Liaison Office CDC Liaison Office D&PS Branch Library
1	Library of Congress Technical Information Division ATTN: Bibliography Section Reference Department Washington 25, D. C.		
1	Carnegie Institute of Technology ATTN: Prof. E. M. Pugh Pittsburgh 13, Pennsylvania		
1	Colorado School of Mines ATTN: Dr. John Rinehart Golden, Colorado		
1	Stanford Research Institute Poulter Laboratories Menlo Park, California		
4	Australian Group c/o Military Attache Australian Embassy 2001 Connecticut Avenue, N. W. Washington, D. C. 20008		
10	The Scientific Information Officer Defence Research Staff British Embassy 3100 Massachusetts Avenue, N. W. Washington, D. C. 20008		

<p>AD Ballistic Research Laboratories, APG SHOCK COMPRESSION OF PLEXIGLAS AND POLYSTYRENE G. E. Hauver and A. Melani</p> <p>BRL Report No. 1259 August 1964 RDT & E Project No. LM014501A33E UNCLASSIFIED Report</p> <p>Hugoniot curves for Plexiglas and polystyrene have been established experimentally using optical and polarization techniques. Both Hugoniot curves show evidence of a phase transition, although the polystyrene transition is more clearly defined than that of Plexiglas. Separate polarization studies support the existence of both transitions. At the transitions, it is noted that the rarefaction velocity becomes equal to the shock velocity. The nature of the transitions is presently unknown.</p>	<p>UNCLASSIFIED</p> <p>Shock waves in plastics Plastics - Hugoniot curves Shock waves - Measurements</p>	<p>AD Ballistic Research Laboratories, APG SHOCK COMPRESSION OF PLEXIGLAS AND POLYSTYRENE G. E. Hauver and A. Melani</p> <p>BRL Report No. 1259 August 1964 RDT & E Project No. LM014501A33E UNCLASSIFIED Report</p> <p>Hugoniot curves for Plexiglas and polystyrene have been established experimentally using optical and polarization techniques. Both Hugoniot curves show evidence of a phase transition, although the polystyrene transition is more clearly defined than that of Plexiglas. Separate polarization studies support the existence of both transitions. At the transitions, it is noted that the rarefaction velocity becomes equal to the shock velocity. The nature of the transitions is presently unknown.</p>	<p>UNCLASSIFIED</p> <p>Shock waves in plastics Plastics - Hugoniot curves Shock waves - Measurements</p>
<p>AD Ballistic Research Laboratories, APG SHOCK COMPRESSION OF PLEXIGLAS AND POLYSTYRENE G. E. Hauver and A. Melani</p> <p>BRL Report No. 1259 August 1964 RDT & E Project No. LM014501A33E UNCLASSIFIED Report</p> <p>Hugoniot curves for Plexiglas and polystyrene have been established experimentally using optical and polarization techniques. Both Hugoniot curves show evidence of a phase transition, although the polystyrene transition is more clearly defined than that of Plexiglas. Separate polarization studies support the existence of both transitions. At the transitions, it is noted that the rarefaction velocity becomes equal to the shock velocity. The nature of the transitions is presently unknown.</p>	<p>UNCLASSIFIED</p> <p>Shock waves in plastics Plastics - Hugoniot curves Shock waves - Measurements</p>	<p>AD Ballistic Research Laboratories, APG SHOCK COMPRESSION OF PLEXIGLAS AND POLYSTYRENE G. E. Hauver and A. Melani</p> <p>BRL Report No. 1259 August 1964 RDT & E Project No. LM014501A33E UNCLASSIFIED Report</p> <p>Hugoniot curves for Plexiglas and polystyrene have been established experimentally using optical and polarization techniques. Both Hugoniot curves show evidence of a phase transition, although the polystyrene transition is more clearly defined than that of Plexiglas. Separate polarization studies support the existence of both transitions. At the transitions, it is noted that the rarefaction velocity becomes equal to the shock velocity. The nature of the transitions is presently unknown.</p>	<p>UNCLASSIFIED</p> <p>Shock waves in plastics Plastics - Hugoniot curves Shock waves - Measurements</p>